Phenotypic lentivirus screens to identify functional single domain antibodies

HHS Public Access

Author manuscript

Nat Microbiol. Author manuscript; available in PMC 2016 December 20.

Published in final edited form as:

Nat Microbiol. ; 1(8): 16080. doi:10.1038/nmicrobiol.2016.80.

Phenotypic lentivirus screens to identify functional single domain antibodies

Florian I. Schmidt[1], **Leo Hanke**[1], **Benjamin Morin**[2,4], **Rebeccah Brewer**[1], **Vesna Brusic**[2], **Sean P.J. Whelan**[2], and **Hidde L. Ploegh**[1,3,*]

[1]Whitehead Institute for Biomedical Research, Cambridge, MA 02142

[2]Department of Microbiology and Immunobiology, Harvard Medical School, Boston, MA, USA

[3]Department of Biology, Massachusetts Institute of Technology, Cambridge, MA 02139

Abstract

Manipulation of proteins is key in assessing their *in vivo* function. While genetic ablation is straightforward, reversible and specific perturbation of protein function remains a challenge. Single domain antibody fragments, such as camelid-derived VHHs, can serve as inhibitors or activators of intracellular protein function, but functional testing of identified VHHs is laborious. To address this challenge, we developed a lentiviral screening approach to identify VHHs that elicit a phenotype when expressed intracellularly. We identified 19 antiviral VHHs that protect human A549 cells from lethal infection with influenza A virus (IAV) or vesicular stomatitis virus (VSV), respectively. Both negative-sense RNA viruses are vulnerable to VHHs uniquely specific for their respective nucleoproteins. Antiviral VHHs prevented nuclear import of viral ribonucleoproteins or mRNA transcription, respectively, and may provide clues for novel antiviral reagents. In principle, the screening approach described here should be applicable to identify inhibitors of any pathogen or biological pathway.

To identify proteins essential to a biological pathway, small molecule inhibitors or activators may be used to manipulate protein function transiently. Alternatively, screens involving mutagenesis, a reduction in levels or complete elimination of gene products are common[1, 2]. As applied to mammalian cells, these methods usually seek to achieve the removal of a protein from its normal biological context. Many proteins are multi-functional, or are components of multi-subunit complexes. Depletion of any single component may cause unexpected phenotypes due to the collapse of entire protein complexes. Small molecule inhibitors often lack specificity[3] and at best can target a fraction of all proteins of interest. The screening of chemically diverse libraries must be paired with sophisticated methods to identify the molecular targets of any hit identified. Antibodies have been used as

*To whom correspondence and request for materials should be addressed: Hidde L. Ploegh (ploegh@wi.mit.edu).

[4]Current address: Agenus Inc., Lexington, MA, USA

AUTHOR CONTRIBUTIONS

F.I.S., L.H., B.M., R.B., and V.B. performed experiments and analyzed the data. S.P.W. gave critical technical advice. F.I.S. and H.L.P. conceived the study and wrote the manuscript.

intracellular perturbants of protein function after microinjection[4] or cytosolic expression of single chain variable antibody fragments[5], but technical challenges have limited their application to few selected cases.

In addition to conventional antibodies, the immune system of camelids generates heavy chain-only antibodies[6]. Their antigen binding site only consists of the variable domain of the heavy chain. This domain can be expressed on its own and is referred to as a VHH or nanobody, an entity that can retain its function in the reducing environment of the cytosol and independent of glycosylation[7]. Many VHHs bind to their targets with affinities comparable to conventional antibodies. VHHs expressed in the cytosol can therefore act as molecular perturbants by occluding interfaces involved in protein-protein interactions, by binding in the active sites of enzymes, or through recognition or stabilization of distinct conformations of their targets[8, 9]. Both phage and yeast display, as well as mass spectrometry in combination with high throughput sequencing, allow the identification of VHHs based on their binding properties[10–12]. Still, the identification of inhibitory VHHs remains a time-consuming process. VHHs obtained through biochemical screening methods must be expressed individually in the relevant cell type to test for the functional consequences of VHH expression. To address this challenge, we developed a phenotypic VHH screening method in living cells.

Results

A functional VHH screen identifies VHHs that block IAV or VSV infection

To identify VHHs that perturb or modulate protein function in living cells, we established a lentiviral screening strategy in which cells are selected based on the phenotype elicited by the VHHs expressed intracellularly. In two independent screens, we have identified VHHs that protect human A549 cells from lethal infection with influenza A virus (IAV) and vesicular stomatitis virus (VSV), negative-sense RNA viruses that replicate in the nucleus and cytosol, respectively.

We immunized two alpacas with inactivated IAV and VSV, isolated peripheral blood lymphocytes, extracted RNA, and amplified VHH coding sequences by PCR using VHH-specific primers (Fig. 1). VHH coding sequences were cloned into a lentiviral vector that allows their expression under a doxycycline (Dox)-inducible promoter in transduced cells. VSV G-pseudotyped lentivirus was produced in 293T cells and used to transduce A549 cells with a multiplicity of infection (MOI) of 0.25 to ensure that cells were not infected by multiple lentivirus particles. Based on the expression of the selection marker neomycin phosphotransferase II, we determined the transduction rate to be 33% in the IAV screen and 55% in the VSV screen (Supplementary Fig. 1), indicating that 81 and 65% of the transduced cells were expected to be infected with a single lentivirus (assuming a Poisson distribution). Following the induction of VHH expression by Dox treatment, the pool of cells was challenged with a lethal dose of IAV (MOI 13) or VSV (MOI 4.5). To increase the stringency of the selection procedure, cells were trypsinized two days post infection because infected cells can stay adherent to tissue culture dishes but do not usually reattach once removed by trypsin treatment. To prevent continuous superinfection with VSV produced by non-VHH protected cells, ammonium chloride was added to the media for the first three

days to prevent the endosomal acidification required for VSV G-mediated virus fusion. Survivors that adhered after trypsinization were grown under carboxymethyl cellulose overlays to prevent diffusion and further spread of VSV. Such precautions were not necessary for the IAV screen, since progeny IAV produced by A549 cells is not infectious unless HA is cleaved by trypsin or other proteases. Cells that survived the virus challenge were cultured for 3–4 weeks and cells were collected as individual colonies, expanded and analyzed.

Each clone of surviving cells was tested individually in a single-round, flow cytometry-based, infection assay in the absence or presence of Dox to see whether infection was blocked by VHH expression. Of 257 of the cell clones obtained from the IAV screen, 166 showed a Dox-dependent reduction of infection by at least 40% (Fig. 2a). In the majority of clones (132), VHH expression reduced infection by more than 80%. 143 of the 282 cell clones obtained from the VSV screen exhibited a Dox-dependent reduction of infection by more than 40%, most of them (127) by more than 80%. A substantial fraction of cell clones that did not meet the hit criteria could no longer be infected even in the absence of Dox, which we attribute to leaky expression of the VHH in the absence of induction, or due to the selection of cell clones that were resistant to infection by genetic abnormalities. We did not pursue these clones further.

VHH coding sequences from clones considered true hits were amplified from purified genomic DNA by PCR, followed by direct sequencing of the PCR product. 68 of the 166 IAV hits contained a single VHH insertion that could unambiguously be sequenced, while 46 of the 143 clones obtained in the VSV screen were the result of a single insertion. For simplicity, cells with multiple lentivirus insertions were omitted from further analysis. The amino acid sequence of the encoded VHHs were compared and clustered by similarity, yielding 15 clusters of VHHs preventing IAV infection (each found between 1 and 12 times), as well as 4 clusters of VHHs preventing VSV infection (Fig. 2b). Strikingly, the cluster including the anti-VSV VHH 1001 was identified in 34 of the 41 independent clones with only slight sequence variations. One of the anti-IAV VHHs, VHH 103 was nearly identical to VHH NP1 that had been identified from a phage display library constructed from the same immunized animal[13]. Of note, 8 of the anti-IAV VHHs contained signatures of V regions of heavy chains of conventional antibodies (V37, G44, L45, E46, and W47 in Fig. 2b), which can be used promiscuously for heavy chain-only antibodies[6, 7, 10]. This phenotypic VHH screen in mammalian cells identified 19 unique VHHs that block infection with IAV or VSV.

Anti-viral activity of identified VHHs

For each of the hits, representative monoclonal cell lines obtained in the screen were further characterized. Cells were infected with IAV and VSV in the absence and presence of Dox (Fig. 3). As controls, we used cell lines that inducibly express VHH NP1[13], a VHH against IAV NP that blocks IAV infection, or VHH HA68[14], a VHH specific for the extracellular portion of IAV HA that does not impair infection with either virus when expressed in the cytosol. To assess IAV infection by flow cytometry, we stained for NP with fluorescently labeled VHH NP2[13], another VHH specific for IAV NP (Fig. 3a). The VSV strain used

expresses EGFP in addition to VSV structural proteins, and infection was therefore quantified by measuring EGFP-positive cells (Fig. 3b). VHH expression was quantified by staining the HA-tagged VHHs (Supplementary Fig. 2). With the exception of VHHs 135, 170, and 355, which reduced IAV infection by 42, 83, and 78%, all IAV hits blocked IAV infection by more than 90%, but did not impair infection with VSV. Vice versa, all VSV hits blocked VSV infection by at least 90%, but allowed IAV infection to proceed to normal levels. Remarkably, almost complete abrogation of infection was in some cases achieved with VHHs expressed at barely detectable levels. To verify that the Dox-dependent resistance to infection indeed depended on the expressed VHH, we transduced A549 cells with lentiviruses that allow inducible expression of the respective VHHs and confirmed their antiviral activity (Supplementary Fig. 3). Specificity of inhibition was thus confirmed unambiguously for the respective virus-specific VHHs

Identification of the targets recognized by antiviral VHHs

The VHH library used for both screens was constructed based on RNA obtained from animals immunized with inactivated virions. The identified antiviral VHHs therefore most likely targeted structural virus proteins. We applied LUMIER assays[15] to test the recognition of viral proteins fused to Renilla luciferase by transiently expressed HA-tagged VHHs. We limited this analysis to virus proteins exposed to the cytosol or nucleus: the polymerase subunits PB2, PB1 and PA, as well as nucleoprotein NP, matrix protein M1, and the ion channel M2 in the case of IAV; the polymerase L, nucleoprotein N, phosphoprotein P, and matrix protein M in the case of VSV. We found that all newly identified anti-IAV VHHs recognized the viral nucleoprotein NP (Fig. 4a), and that anti-VSV VHHs targeted the viral nucleocapsid N (Fig 4c). These findings suggest that viral RNA binding proteins represent an underappreciated vulnerability of negative-stranded RNA viruses. To efficiently block infection, antiviral VHHs may have to target incoming viruses at an early step of the life cycle, which may have biased the screening results towards VHHs that target components of incoming vRNPs. The exclusive identification of antiviral NP- and N-binders likely also reflects the abundance of the respective proteins in the virions used for immunization.

We expressed the virus-specific VHHs in bacteria and tested the extent to which the purified VHHs compete for epitopes on IAV NP and VSV N. For competition assays, purified NP or N was pre-incubated with an excess of His_6-tagged VHHs. VHHs site-specifically biotinylated by means of a sortase reaction[16] were then used for co-precipitation experiments with streptavidin-coupled beads. NP or N was recovered by the biotinylated VHH, unless pre-incubation with an unlabeled VHH masked the epitope recognized by the biotinylated VHHs.

We could thus categorize the IAV NP-binding VHHs into three groups (Fig. 4b): Group I included VHH 103, Group II included VHHs 22 and 495, and Group III was comprised of VHHs 28, 52, 77, 108, 135, 151, 170, 191, 296, 341, 355, and 508. VHH NP2, a VHH specific for IAV NP identified previously[13] and used to quantify IAV infection, did not compete with any of the VHHs identified in this screen (Supplementary Fig. 4).

Binding of the VSV N-specific VHHs 1001, 1004, and 1014 was not affected by any of the other VSV N VHHs, including VHH 1307 (Fig. 4d). Immunoprecipitation of N by VHH

1307, however, was impaired by preincubation with VHH 1014, although the reverse setup allowed successful co-immunoprecipitation of N and the His-tagged VHH. This suggests that 1001, 1004, and 1014 bind to separate epitopes of VSV N, while 1307 may bind to an epitope that is partially overlapping with VHH 1014 or altered by binding of VHH 1014.

Anti-IAV VHHs block nuclear import of vRNPs and viral mRNA transcription

We next sought to define the step of the viral replication cycle at which the anti-IAV VHHs block infection. After fusion of the viral membrane with that of late endosomes, viral ribonucleoproteins (vRNPs) are released into the cytosol, followed by import into the nucleus to allow replication and transcription of viral RNAs. To quantify nuclear import of vRNPs, we infected VHH-expressing cell lines with a high MOI of IAV in the presence of cycloheximide to block translation of new viral proteins. We then determined the localization of incoming vRNPs by confocal fluorescence microscopy (Fig. 5). NP predominantly localized to the nucleus in untreated A549 cells and in cells expressing the control VHH HA68. Treatment of A549 cells with bafilomycin A1, an inhibitor of the endosomal vATPase, blocks endosomal acidification and virus fusion, and thus nuclear import of vRNPs – causing an absence of nuclear NP staining. To quantify nuclear import in VHH-expressing cells, we calculated the ratio of NP signal strength in the nucleus and in the cytoplasm, and determined relative nuclear import by comparison with untreated cells (relative nuclear import = 1) and cells treated with bafilomycin A1 (relative nuclear import = 0). With the exception of VHH 170, all VHHs blocked nuclear import substantially, with relative nuclear import values ranging from 0 to 0.5. Binding of VHHs to NP must impair binding of importins to vRNPs, inhibit translocation of vRNPs through the nuclear pore complex, or interfere with an unknown step that precedes nuclear import *per se*. The VHH expressors were challenged with a very high dose of virus: the respective VHHs must therefore be capable of potently blocking nuclear import, for some VHHs even when expressed at a relatively low level (Supplementary Fig. 2). It is possible that the effects of VHH 170 on nuclear import were overcome in the experimental setup used.

Inhibition of vRNP nuclear import likely explains the antiviral properties of the identified anti-IAV VHHs, but it is possible that NP-specific VHHs perturb other functions of the viral nucleoprotein. Following nuclear import of vRNPs, the viral RNA polymerase transcribes the viral genomic segments and replicates the viral RNA genomes (vRNA). NP associates with vRNA and complementary RNA (cRNA), and is essential for complete replication and transcription of viral RNA by IAV polymerase[17]. We therefore used a minigenome replication assay, in which polymerase activity is assessed in the absence of a natural infection: The viral RNA polymerase subunits PB2, PB1, and PA as well as NP and the respective VHHs were transiently expressed in the presence of a model IAV genome segment encoding EGFP (Fig. 5c and 5d). Viral mRNAs encoding EGFP were transcribed from the model genome and translated. EGFP expression required the presence of NP as well as each RNA polymerase subunit (Supplementary Fig. 6), but is not expected to rely on the nuclear import of vRNPs, which we have shown to be sensitive to antiviral VHHs. Most of the antiviral VHHs and the control VHH HA68 did not perturb viral gene expression. This suggests that the binding of a VHH to vRNP templates is in principle compatible with transcription, at least at the ratio of NP and VHHs achieved in the experimental setup.

However, VHHs 22, 151, and 495 substantially reduced RNA polymerase activity. We thus identified three VHHs that bind to NP epitopes crucial for NP-dependent RNA polymerase activity. VHHs 22 and 495, while distinct in sequence, exhibit similar CDRs and bind to overlapping epitopes on NP, confirming the functional importance of this binding site. None of the expressed VHHs prevented nuclear import of free NP (Supplementary Fig. 5).

In summary, we found that 14 of the 15 newly identified IAV NP-specific VHHs block nuclear import of incoming vRNPs, and that at least three of these also block NP-dependent viral RNA polymerase activity. Our functional VHH screen therefore discloses vulnerabilities of IAV NP that may represent druggable targets.

Anti-VSV VHHs block viral mRNA transcription

In the course of VSV entry, viral membranes fuse with limiting membranes of early endosomes to release the viral genomes with associated proteins into the host cell cytosol. The genomes are coated by the nucleocapsid protein N (N-RNA) and are associated with the polymerase L, bound through its co-factor P. N-RNA serves as a template for polymerase-catalyzed mRNA transcription, which involves transcription of an uncapped leader sequence, followed by transcription of five capped and polyadenylated mRNA species, all catalyzed by the multifunctional RNA polymerase[18–20].

To quantify mRNA transcription directly, we infected the VHH-expressing cell lines with VSV and metabolically labelled the produced RNA species with [^{3}H]-uridine (Fig. 6a,b). While all five mRNA species could be detected in the absence of VHH expression, mRNA was undetectable in VSV-infected cells expressing VHH 1001, 1004, and 1307, and substantially reduced in cells expressing VHH 1014. This confirms that anti-VSV VHHs prevent viral gene expression by directly or indirectly blocking mRNA transcription.

The viral mRNAs detected in infected cells are the products of both primary transcription from incoming viral genomes and transcription from replicated genomes. To specifically analyze primary transcription, we performed *in vitro* polymerase assays in the absence and presence of VHHs using purified components, including N-RNA templates obtained from virions[21, 22] (Fig. 6c). At a ratio of 10 molecules of VHH per 63 molecules of N, the maximum concentration at which all VHHs remained soluble, VHH 1001 and 1307 abrogated RNA transcription almost completely, while VHH 1004 and 1014 did not substantially block RNA transcription. The lack of inhibition by VHH 1004 and 1014 could be attributed to 1) a binding site on N that allows transcription in the presence of substoichiometric levels of VHH, 2) lower affinity of the VHHs to N, or 3) the fact that the respective VHHs target a step that is not recapitulated in the *in vitro* assay, for example genome replication. Exclusive binding of VHHs to newly generated N during infection in cells could directly perturb genome replication and therefore reduce mRNA transcription by decreasing the amount of template.

In sum, all anti-VSV VHHs block viral mRNA transcription by binding to the nucleoprotein N. At substoichiometric levels, VHH-binding to different epitopes of N impaired polymerase activity to variable degrees, suggesting that different mechanisms of action apply. The exact binding sites may hold clues to potential antiviral drugs targeting RNA transcription.

Discussion

The perturbation of molecular processes in the cell has mostly relied on methods that involve genetic intervention (gene knockout, mutagenesis, or knock-down) or the application of small molecule compounds as inhibitors or activators. The available arsenal of well-defined pharmacological inhibitors to reversibly interfere with protein function level is small and mostly limited to 'druggable' proteins. Many such compounds were discovered serendipitously and their specificity is not always easy to establish. The approach described here allows the functional screening of camelid single domain antibodies to identify highly specific gain and loss of function molecular perturbants. Provided a suitable assay is at hand, VHHs can be identified as inhibitors or modulators of any biological process by such phenotypic screens. VHHs can then be inducibly expressed to perturb protein function in a highly specific and reversible manner and thus present a valuable research tool orthogonal to genetic ablation.

The use of VHH libraries from animals immunized with a distinct set of desired protein targets substantially increases the likelihood of obtaining the desired antibody fragments. Large numbers of candidates can be tested in lentiviral screens, an approach that could perhaps be applied to synthetic libraries as well. To identify VHHs, the cytosolic expression of which blocks pathogen infection, it may even be sufficient to harvest the VHH repertoire from a naturally infected animal. Selection of VHHs is not limited to lethal screens, but can be extended to fluorescence-activated cell sorting (FACS) and other enrichment strategies following reporter gene expression or turnover of fluorogenic substrates. There is no reason why the selected phenotypes should be limited to functional perturbation in the cytosol, and similar screens may exploit expression of VHHs targeted to other organelles or rely on display of VHHs at the cell surface. Although we selected and amplified clonal cell lines from cells that survived the screens, high throughput sequencing methods could be used instead to identify enriched VHHs. This approach would be compatible with selection of VHHs in terminally differentiated cells or in cells that have to be fixed prior to cell sorting.

In the screen described here, we identified 19 VHHs that specifically block infection of cells with IAV or VSV. Previous attempts to identify virus specific VHHs using phage display with VHH libraries from the same animals yielded fewer hits that inhibited infection less potently[13]. The screening approach described here thus complements other VHH screening techniques based on affinity, and is likely to be better at identifying VHH-based intracellular inhibitors or activators. The identification of epitopes, the occlusion of which blocks the infectious cycle, may inform the development of small molecule inhibitors, in particular if they are well conserved among different serotypes of a virus. In theory, antiviral application of VHHs fused to cell-penetrating peptides is conceivable as well[23]. These anti-viral VHHs should further help elucidate the vulnerable steps of the viral life cycle. Ongoing structural analysis of the anti-IAV VHHs bound to NP may shed light on how incoming vRNPs are imported into the nucleus and how NP interacts with the necessary cellular factors. Structures of VHHs capable of inhibiting IAV RNA polymerase activity will help unravel how NP contributes to the formation of full length viral mRNA, vRNA, and cRNA transcripts. Similarly, VHHs that target VSV N will be helpful in the molecular analysis of VSV RNA polymerase activity. The finding here that VHHs have different inhibition

properties on *in vitro* transcription and the synthesis of RNA in cells indicates that such tools may well aid in the discrimination of N-related functions in transcription vs replication. Of note, homologues of the VSV polymerase and nucleocapsid are found in many human pathogens of the order mononegavirales, including rabies virus, Ebola virus, mumps virus, measles virus, and respiratory syncytial virus (RSV)[24].

Methods

Cell lines

Human epithelial A549 and HEK 293T cells, canine MDCK cells, and hamster BHK-21 cells were obtained from ATCC and grown in DMEM supplemented with 10% FBS. A549 cell lines inducibly expressing HA-tagged VHHs were cultivated in the presence of 500 μg/mL geneticin. All cell lines used for experiments were negative for *Mycoplasma* as judged by the absence of of cytosolic Hoechst 33342-positive foci in immunofluorescence microscopy samples.

Virus

A/WSN/33 strain of influenza virus was propagated in MDCK cells in the presence of trypsin and concentrated by sedimentation (75,000 g, 4° C, 2h) through a 20% sucrose cushion (in 20 mM Tris pH 7.6, 150 mM NaCl), followed by resuspension in desorption buffer (0.245% BSA in 20 mM Tris pH 7.6, 150 mM NaCl). VSV Indiana and VSV Indiana GFP were propagated in BHK-1 cells. Clarified supernatants were used for flow cytometry-based infection assays.

Reagents

Doxycycline hyclate (Dox) was purchased from Sigma Aldrich. Hybridoma cells secreting mouse monoclonal anti-IAV NP (clone H16-L10-4R5, ATCC HB-65)[25] were obtained from ATCC and antibodies in the supernatant purified using a protein G column. Polyclonal rabbit anti-neomycin phosphotransferase II (NPTII) was purchased from Fitzgerald Industries International. Mouse anti-HA.11 (clone 16B12) was acquired from BioLegend, polyclonal rabbit anti-HA (Y-11) from Santa Cruz. Mouse anti-HA.11 (clone 16B12) coupled to Alexa Fluor (AF) 488 or AF594, as well as fluorescently-labeled secondary antibodies and AF647 Phalloidin were obtained from Life Technologies.

Generation of lentiviral plasmid VHH library

In order to raise heavy chain-only antibodies against structural components of IAV and VSV, two male alpacas were immunized five times with a mixture of ethanol-inactivated IAV PR8 and VSV Indiana (ca. 10^{12} plaque forming units of each virus per injection) according to a protocol authorized by the Tufts University Cummings Veterinary School Institutional Animal Care and Use Committee. RNA from peripheral blood lymphocytes was extracted and used as a template to generate cDNA using three sets of primers (random hexamers, oligo(dT), and primers specific for the constant region of the alpaca heavy chain gene)[10, 26]. VHH coding sequences were amplified by PCR using VHH-specific primers, cut with NotI and AscI, and ligated into the M13 phagemid vector pJSC to yield the VHH phagemid plasmid library described in our previous study[13]. A derivative of pInducer20[27], pInducer20-

NA, was generated by removing all NotI restriction sites and by replacing the gateway cassette with a DNA fragment containing NotI and AscI restriction sites. VHHs were subcloned into pInducer20-NA and the library amplified in electroporation competent *Escherichia coli* (*E. coli*) ElectroTen-Blue while maintaining the diversity of the phagemid library ($2.4 \cdot 10^7$ ampicillin-resistant colonies obtained).

Generation of lentivirus library

Lentiviral particles were generated by transfecting HEK 293T cells in 15 cm dishes with psPax2, pMD2.G (both kind gifts from Didier Trono, École polytechnique fédérale de Lausanne, Switzerland), and the pInducer20-NA VHH library using Lipofectamine 2000 (Life Technologies). Supernatants were harvested 48 h post transfection and filtered through 0.4 μm filters. Virus stocks were titered on A549 cells by flow cytometry using anti-NPII, goat anti-rabbit AF647 and a BD Biosciences LSRFortessa flow cytometer.

Lentivirus VHH screen

A549 cells in 15 cm dishes were transduced with the lentivirus library at a multiplicity of infection (MOI) of 0.25 in the presence of 10 μg/mL polybrene. VHH expression was induced 8 h post transduction by the addition of Dox to a final concentration of 1 μg/mL. 48 h post transduction, cells were infected with IAV/WSN/33 in DMEM (0.2% BSA) at an MOI of 13 or VSV EGFP Indiana in DMEM at an MOI of 4.5. The inoculum was removed 1 h post infection and cells were covered with fresh DMEM containing 10% FBS, 1 μg/mL Dox, Penicillin/Streptomycin, and Fungizone Antimycotic (Life Technologies); medium of VSV-infected cells was supplemented with 100 mM NH_4Cl and 20 mM Hepes. 48 h post infection with IAV or VSV, cells were washed with PBS, trypsinized, split 1:2, and seeded in DMEM with 20% FBS, 1 μg/mL Dox, Penicillin/Streptomycin, and Fungizone Antimycotic (as well as 100 mM NH_4Cl and 20 mM Hepes in case of VSV-infected cells). The medium of the IAV plates was replaced every 2–3 days until most cells had detached. Adherent cells of the VSV plates were covered with DMEM containing 1.5% carboxymethyl cellulose, 20% FBS, 500 μg/mL G418, 1 μg/mL Dox, Penicillin/Streptomycin, and Fungizone Antimycotic and left unperturbed. 3–4 weeks later, cell colonies were harvested from the plates, individually amplified, tested in infection assays, and frozen. To prevent infection of cell clones with residual VSV, freshly picked clones of the VSV screen were grown in 1.5 μg/mL VSV-neutralizing antibody IE2[28] and controlled for EGFP expression. To retrieve the VHH sequences encoded by surviving cell clones, we lysed cells in 1% SDS, 50 mM Tris, 100 mM NaCl, 1 mM EDTA, 100 μg/mL proteinase K at 55°C for 2h. Genomic DNA was subsequently precipitated by addition of one volume of isopropanol, dried in a fume hood, and resuspended in ddH_2O. VHH sequences were amplified with lentivirus-specific primers using the Platinum PCR Super Mix (Life Technologies) and directly sequenced from PCR products. VHH sequences were analyzed by ClustalW alignment, and neighbor-joining trees were constructed to group identical or highly similar sequences (<3 aa differences in CDRs). One representative sequence of each group was chosen for further analysis. The antiviral VHH sequences were deposited in the NCBI GenBank sequence data base with the accession numbers KX022606-KX022624.

Flow cytometry-based infection assays

To quantify infection by flow cytometry, A549 cell lines were seeded in 24-well plates 40 h before infection ($2{\cdot}10^4$ cells/well). Cells were treated with 1 μg/mL Dox 24 h before infection to induce VHH expression. Cells were infected with appropriate amounts of IAV WSN/33 (in 0.2% BSA/DMEM) or VSV Indiana GFP (in DMEM) to infect 50% of wild-type cells. 30 minutes post infection, inocula were removed and cells cultivated for 5:30 h (IAV) or 3:30 h (VSV) in full medium. Cells were trypsinized, fixed in 4% formaldehyde/PBS, and stained with 100 ng/mL AF647-coupled VHH NP2 and mouse anti-HA AF488 (IAV-infected cells), or mouse anti-HA AF594 (VSV-infected cells), all under permeabilizing conditions. Fluorescence was quantified using a BD Biosciences LSRFortessa flow cytometer and the FlowJo software package.

LUMIER Assay

Protein interactions in transfected HEK 293T cells were quantified using the LUMIER assay according to a protocol modified from Taipale *et al.*[29]. HEK 293T cells in 24-wells were transfected with 0.25 μg bait expression vectors (pCAGGS VHH-HA) and 0.25 μg prey expression vectors (IAV: empty vector, pEXPR PB2-Renilla, pEXPR PB1-Renilla, pEXPR PA-Renilla, pEXPR Renilla-NP, pEXPR Renilla-M1, or pEXPR M2-Renilla; VSV: empty vecor, pEXPR N-Renilla, pEXPR Renilla-P, pEXPR Renilla-M, pEXPR Renilla-L, pEXPR Renilla-L_N, or pEXPR Renilla-L_C; all expression vectors are derived from pcDNA3-ccdB-Renilla, a kind gift of Mikko Taipale, Susan Lindquist laboratory, Whitehead Institute, Cambridge, MA, USA) using Lipofectamine 2000. 24 h post transfection, cells were lysed in 120 μL LUMIER IP buffer (50 mM Hepes pH 7.9, 150 mM NaCl, 2 mM EDTA pH 8.0, 0.5% Triton X-100, 5% glycerol, protease inhibitor cocktail (Roche)). 90 μL of the lysates were transferred to blocked LUMITRAC™ 600 plates (Greiner) coated with mouse anti-HA. 11 and incubated at 4°C for 3 h. After extensive washing steps with IP buffer, incubated wells (or 10 μL lysate) were incubated with Coelenterazine-containing Renilla luciferase substrate mix (BioLux Gaussia Luciferase Assay Kit, New England BioLabs) and light emission quantified using a SpectraMax M3 microplate reader (Molecular Devices). Renilla luciferase activity in the immunoprecipitation samples was normalized by Renilla luciferase activity in the lysates.

Protein Expression and Purification

For periplasmic bacterial expression, VHH coding sequences were cloned into a derivative of pHEN6[30] encoding a C-terminal sortase recognition site (LPETG) followed by a His_6-tag. VHH-LPETG-His_6 fusion proteins were expressed in *E. coli* WK6 cells and purified from periplasmic extracts using Ni-NTA affinity purification and size exclusion chromatography with a HiLoad 16/600 Superdex 75 pg column. To fluorescently label or biotinylate VHHs using sortase, proteins were incubated with sortase and GGG-Alexa Fluor 647 or GGG-biotin as described before (Guimaraes et al., 2013), followed by removal of His-tagged sortase with Ni-NTA beads and desalting.

The IAV/WSN/33 NP cds was cloned into pET30b+. NP-His_6 was expressed in *E. coli* LOBSTR[31] and purified by Ni-NTA purification, Mono S cation exchange chromatography, and size exclusion chromatography with a HiLoad 16/60 Superdex 200 column. VSV

Indiana N was purified as described before[32]. In brief, *E. coli* BL21(DE3) was transformed with pET N/P to co-express VSV N and P protein. The N/P complex associated with RNA was purified by Ni-NTA purification, P precipitated during dialysis against an acidic buffer (100 mM citrate, pH 4.0, 250 mM NaCl), and N-RNA further purified by gel filtration with a HiLoad 16/60 Superdex 200 column.

Competition assays

Immunoprecipitations for competition assays were performed with 2 μg C-terminally biotinylated VHH[16] bound to streptavidin magnetic beads (MyOne Dynabeads; Life Technologies) and 7.5 μg of recombinant IAV WSN NP. Before addition to the beads, NP was blocked with 50 μg of the individual His-tagged VHHs. Bound NP was eluted in 0.2 M glycine, pH 2.2, and analyzed by SDS-PAGE and colloidal Coomassie staining. The complete gels corresponding to Fig. 4 and Supplementary Fig. 4 are displayed in Supplementary Fig. 7.

IAV vRNP nuclear import assay

To quantify nuclear import of vRNPs, A549 cell lines were seeded in 24-well plates 40 h before infection (10^4 cells/well). Cells were treated with 1 μg/mL Dox 24 h before infection to induce VHH expression. IAV WSN/33 (in 0.2% BSA/DMEM) at an MOI of 230 was bound to the cells on ice for 1h in the presence of 1 mM cycloheximide (CHX). Cells were subsequently covered with fresh BSA/DMEM with CHX and incubated at 37° C for 4 h. Cells were fixed with 4% formaldehyde and permeabilized in permeabilisation buffer (PS) (0.05% saponin, 1% BSA, 0.05% NaN_3 in PBS) for 20 min. Samples were incubated with mouse anti-NP (clone HB-65, 1 μg/mL in PS) and rabbit anti-HA (1:200 in PS) for 2 h, washed with PBS, and subsequently incubated with AF488-coupled goat anti-mouse IgG and AF594-coupled goat anti-rabbit IgG (both 1:1,000 in PS), Hoechst 33342 (1:5,000), and AF647 Palloidin (1:100) for 1 h. Samples were washed with PBS and H_2O, and mounted with Fluoromount-G (Southern Biotech). Z stacks were acquired using a PerkinElmer Ultraview Spinning Disk Confocal microscope and Z projections from 3 fields of view with a 40x objective (typically containing ca. 50 cells) were analyzed using CellProfiler[33]. Gaussian filters were applied to the DNA and actin channels, which were subsequently used to segment nuclei and cells, respectively. For each cell, the mean intensity of the NP signal in the nucleus was divided by the mean intensity of the NP signal in the cytoplasm. Average values for all cells in one experimental condition were calculated and normalized to the values for untreated A549 cells (nuclear import = 1.0) and BafA-treated cells (nuclear import = 0).

IAV minigenome replication assay

To quantify polymerase activity of transiently expressed IAV polymerase, 293T cells were transfected with 150 ng of each pCAGGS PB2, pCAGGS PB1, pCAGGS PA, pCAGGS NP[34], pPolI-EGFP-RT (a derivative of pPolI-NS-RT[35] in which the NS coding sequence was replaced with EGFP, and which allowed transcription of the model IAV genome segment by host cell RNA polymerase I), and the respective pCAGGS VHH-HA vector (or empty vector) using Lipofectamine 2000. 24 h post transfection, cells were fixed and stained with AF594 mouse anti-HA. VHH-HA expression was measured and EGFP fluorescence in HA-

positive cells quantified using a BD Biosciences LSRFortessa flow cytometer and the FlowJo software package.

VSV mRNA transcription assay in infected cells

To analyze viral RNA species in infected cells, A549 cell lines were seeded in 60 mm dishes and, where indicated, VHH expression induced with 1 μg/mL Dox for 24 h hours. 85% confluent cells were infected with VSV at an MOI of 100 in 1 ml of DMEM with 1 μg/ml of Dox (where indicated). After 45 min at 34° C, 2 ml of DMEM complemented with 60 μl actinomycin D (0.5 mg/ml), 50 μl of [5,6-^{3}H]-Uridine (38 Ci/mmol, Moravek Biochemicals) and 1 μg/ml of Dox (where indicated) were added to the cells. After 5 h of incubation at 34° C, cytoplasmic extracts were prepared and RNA was purified by phenol/chloroform extraction as described previously[36]. Purified RNA extracts were analyzed by acid/agarose gel electrophoresis and autoradiography[37]. The complete autoradiograph corresponding to Fig. 6a is displayed in Supplementary Fig. 7.

VSV *in vitro* transcription assay

Genomic N-RNA templates were prepared from VSV virions as previously described[21]. Polymerase assays were carried out as described[38] using 0.25 μg of N-RNA with 0.2 μM of VSV L and 0.3 μM of VSV P in a reaction mixture containing 20 mM Tris, pH 8.0, 50 mM NaCl, 6 mM MgCl2, 500 μM UTP, 250 μM GTP, 1 mM ATP, 1 mM CTP, 165 nM of [α^{32}P]-GTP (3000 Ci/mmol) (Perkin-Elmer) and, where indicated, 80 μM of the respective VHHs. Reactions were incubated at 30° C for 2.5 h and stopped by addition of EDTA/formamide. Reactions products were resolved using acid/agarose gel electrophoresis and autoradiography[37]. The complete autoradiograph corresponding to Fig. 6c is displayed in Supplementary Fig. 7.

Supplementary Material

Refer to Web version on PubMed Central for supplementary material.

Acknowledgments

We thank Brian Bierie for help with lentiviral vectors, Mikko Taipale and Georgios Karras for help with LUMIER assays, Sarah Hulsey Stubbs for VSV-neutralizing antibodies, and Tom DiCesare for help with illustrations. This work is supported by a National Institutes of Health Pioneer award to H.L. Ploegh and additional funding from Fujifilm/MediVector; F.I.S. was supported by an Advanced Postdoc.Mobility Fellowship from the Swiss National Science Foundation (SNSF).

References

1. Mohr SE, Smith JA, Shamu CE, Neumuller RA, Perrimon N. RNAi screening comes of age: improved techniques and complementary approaches. Nat Rev Mol Cell Biol. 2014; 15:591–600. [PubMed: 25145850]
2. Kim H, Kim JS. A guide to genome engineering with programmable nucleases. Nature reviews Genetics. 2014; 15:321–334.
3. Cohen P. Guidelines for the effective use of chemical inhibitors of protein function to understand their roles in cell regulation. Biochem J. 2010; 425:53–54. [PubMed: 20001962]
4. Doxsey SJ, Brodsky FM, Blank GS, Helenius A. Inhibition of endocytosis by anti-clathrin antibodies. Cell. 1987; 50:453–463. [PubMed: 3111717]

5. Gargano N, Cattaneo A. Rescue of a neutralizing anti-viral antibody fragment from an intracellular polyclonal repertoire expressed in mammalian cells. FEBS Lett. 1997; 414:537–540. [PubMed: 9323030]
6. Hamers-Casterman C, et al. Naturally occurring antibodies devoid of light chains. Nature. 1993; 363:446–448. [PubMed: 8502296]
7. Muyldermans S. Nanobodies: natural single-domain antibodies. Annu Rev Biochem. 2013; 82:775–797. [PubMed: 23495938]
8. Helma J, Cardoso MC, Muyldermans S, Leonhardt H. Nanobodies and recombinant binders in cell biology. J Cell Biol. 2015; 209:633–644. [PubMed: 26056137]
9. Schmidt FI, et al. A Single Domain Antibody Fragment that Recognizes the Adaptor ASC Defines the Role of ASC Domains in Inflammasome Assembly. J Exp Med. 2016; 213:771–790. [PubMed: 27069117]
10. Maass DR, Sepulveda J, Pernthaner A, Shoemaker CB. Alpaca (Lama pacos) as a convenient source of recombinant camelid heavy chain antibodies (VHHs). Journal of immunological methods. 2007; 324:13–25. [PubMed: 17568607]
11. Ryckaert S, Pardon E, Steyaert J, Callewaert N. Isolation of antigen-binding camelid heavy chain antibody fragments (nanobodies) from an immune library displayed on the surface of Pichia pastoris. Journal of biotechnology. 2010; 145:93–98. [PubMed: 19861136]
12. Fridy PC, et al. A robust pipeline for rapid production of versatile nanobody repertoires. Nature methods. 2014; 11:1253–1260. [PubMed: 25362362]
13. Ashour J, et al. Intracellular expression of camelid single-domain antibodies specific for influenza virus nucleoprotein uncovers distinct features of its nuclear localization. J Virol. 2015; 89:2792–2800. [PubMed: 25540369]
14. Dougan SK, et al. Antigen-specific B-cell receptor sensitizes B cells to infection by influenza virus. Nature. 2013; 503:406–409. [PubMed: 24141948]
15. Barrios-Rodiles M, et al. High-throughput mapping of a dynamic signaling network in mammalian cells. Science. 2005; 307:1621–1625. [PubMed: 15761153]
16. Guimaraes CP, et al. Site-specific C-terminal and internal loop labeling of proteins using sortase-mediated reactions. Nat Protoc. 2013; 8:1787–1799. [PubMed: 23989673]
17. Fodor E. The RNA polymerase of influenza a virus: mechanisms of viral transcription and replication. Acta virologica. 2013; 57:113–122. [PubMed: 23600869]
18. Lyles, DS.; Rupprecht, CE. Fields' Virology. Fields, BN.; Knipe, DM.; Howley, PM., editors. Wolters Kluwer Health/Lippincott Williams & Wilkins; Phila: 2007. p. 1364-1408.
19. Emerson SU, Wagner RR. Dissociation and reconstitution of the transcriptase and template activities of vesicular stomatitis B and T virions. J Virol. 1972; 10:297–309. [PubMed: 4342247]
20. Green TJ, Luo M. Structure of the vesicular stomatitis virus nucleocapsid in complex with the nucleocapsid-binding domain of the small polymerase cofactor, P. Proc Natl Acad Sci U S A. 2009; 106:11713–11718. [PubMed: 19571006]
21. Rahmeh AA, et al. Molecular architecture of the vesicular stomatitis virus RNA polymerase. Proc Natl Acad Sci U S A. 2010; 107:20075–20080. [PubMed: 21041632]
22. Baltimore D, Huang AS, Stampfer M. Ribonucleic acid synthesis of vesicular stomatitis virus, II. An RNA polymerase in the virion. Proc Natl Acad Sci U S A. 1970; 66:572–576. [PubMed: 4317920]
23. Li T, et al. Cell-penetrating anti-GFAP VHH and corresponding fluorescent fusion protein VHH-GFP spontaneously cross the blood-brain barrier and specifically recognize astrocytes: application to brain imaging. FASEB journal : official publication of the Federation of American Societies for Experimental Biology. 2012; 26:3969–3979. [PubMed: 22730440]
24. Morin B, Kranzusch PJ, Rahmeh AA, Whelan SP. The polymerase of negative-stranded RNA viruses. Current opinion in virology. 2013; 3:103–110. [PubMed: 23602472]
25. Yewdell JW, Frank E, Gerhard W. Expression of influenza A virus internal antigens on the surface of infected P815 cells. J Immunol. 1981; 126:1814–1819. [PubMed: 7217668]
26. Sosa BA, et al. How lamina-associated polypeptide 1 (LAP1) activates Torsin. eLife. 2014; 3:e03239. [PubMed: 25149450]

27. Meerbrey KL, et al. The pINDUCER lentiviral toolkit for inducible RNA interference in vitro and in vivo. Proc Natl Acad Sci U S A. 2011; 108:3665–3670. [PubMed: 21307310]
28. Lefrancois L, Lyles DS. The interaction of antibody with the major surface glycoprotein of vesicular stomatitis virus. I. Analysis of neutralizing epitopes with monoclonal antibodies. Virology. 1982; 121:157–167. [PubMed: 18638751]
29. Taipale M, et al. Quantitative analysis of HSP90-client interactions reveals principles of substrate recognition. Cell. 2012; 150:987–1001. [PubMed: 22939624]
30. Conrath KE, et al. Beta-lactamase inhibitors derived from single-domain antibody fragments elicited in the camelidae. Antimicrob Agents Chemother. 2001; 45:2807–2812. [PubMed: 11557473]
31. Andersen KR, Leksa NC, Schwartz TU. Optimized E. coli expression strain LOBSTR eliminates common contaminants from His-tag purification. Proteins. 2013; 81:1857–1861. [PubMed: 23852738]
32. Green TJ, et al. Access to RNA encapsidated in the nucleocapsid of vesicular stomatitis virus. J Virol. 2011; 85:2714–2722. [PubMed: 21177817]
33. Kamentsky L, et al. Improved structure, function and compatibility for CellProfiler: modular high-throughput image analysis software. Bioinformatics. 2011; 27:1179–1180. [PubMed: 21349861]
34. Schickli JH, et al. Plasmid-only rescue of influenza A virus vaccine candidates. Philosophical transactions of the Royal Society of London. Series B, Biological sciences. 2001; 356:1965–1973. [PubMed: 11779399]
35. Fodor E, et al. Rescue of influenza A virus from recombinant DNA. J Virol. 1999; 73:9679–9682. [PubMed: 10516084]
36. Pattnaik AK, Wertz GW. Replication and amplification of defective interfering particle RNAs of vesicular stomatitis virus in cells expressing viral proteins from vectors containing cloned cDNAs. J Virol. 1990; 64:2948–2957. [PubMed: 2159555]
37. Lehrach H, Diamond D, Wozney JM, Boedtker H. RNA molecular weight determinations by gel electrophoresis under denaturing conditions, a critical reexamination. Biochemistry. 1977; 16:4743–4751. [PubMed: 911786]
38. Morin B, Rahmeh AA, Whelan SP. Mechanism of RNA synthesis initiation by the vesicular stomatitis virus polymerase. The EMBO journal. 2012; 31:1320–1329. [PubMed: 22246179]
39. Cherry S, et al. Genome-wide RNAi screen reveals a specific sensitivity of IRES-containing RNA viruses to host translation inhibition. Genes & development. 2005; 19:445–452. [PubMed: 15713840]

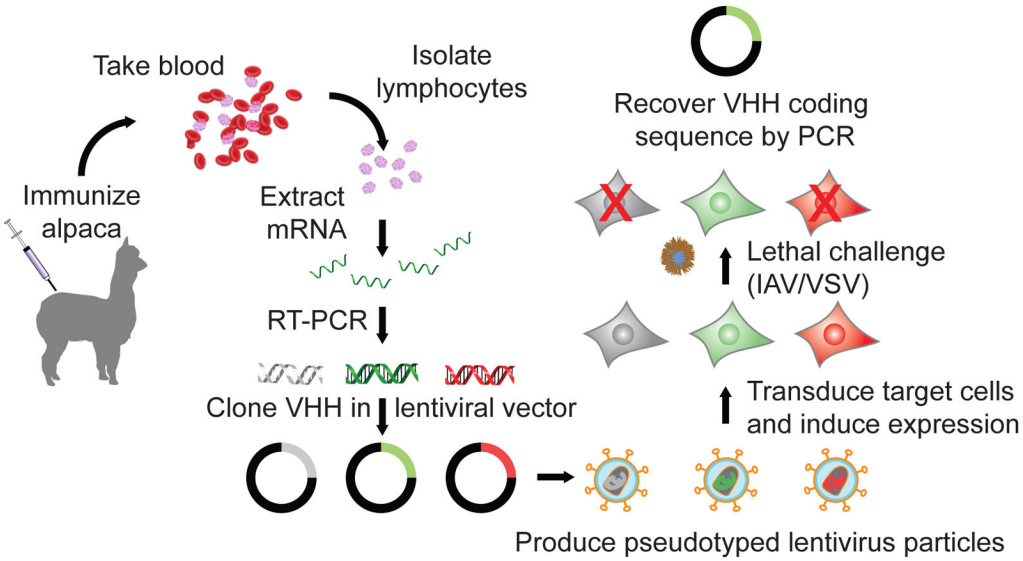

Figure 1.

Lentiviral screening approach. Alpacas are immunized with the desired antigen mix (here: inactivated influenza A virus, IAV, and vesicular stomatitis virus, VSV). After repeated immunizations, we draw a blood sample, purify lymphocytes, extract mRNA, reversely transcribe RNA to cDNA, amplify VHH coding sequences and clone them into a lentiviral vector. Alternatively, VHH coding sequences can be subcloned from an existing VHH library. 293T cells are transfected with the lentiviral library as well as packaging vectors, and lentivirus is harvested from the supernatant 2 days later. We transduce the cell line of interest (here: A549 cells) and induce VHH expression with doxycycline. Cells are then subjected to a selection assay that allows identification of cells expressing the desired VHHs (here: survival of a lethal infection with IAV or VSV). Finally, we prepared genomic DNA from selected (surviving) cells, amplified the VHH sequences by PCR and determined the VHH sequence encoded.

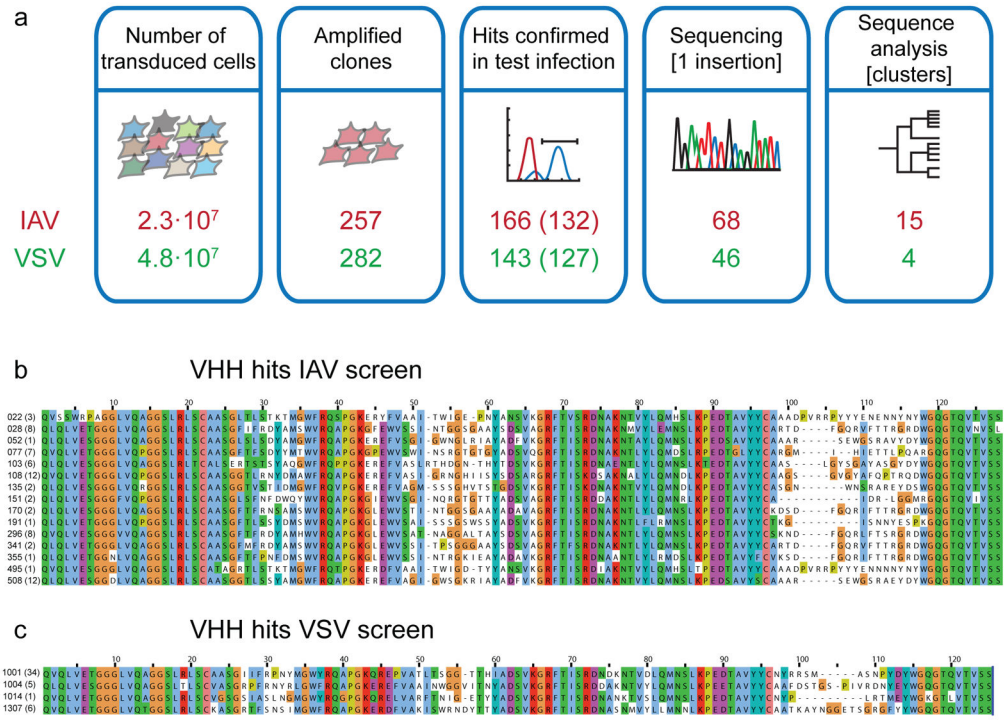

Figure 2.

Overview of the antiviral VHH screen hits. **(a)** Summary of the number of transduced cells, amplified cell clones, number of confirmed hits reducing infection by more than 40% (80%), number of hits containing a single insertion, and number of different VHH clusters in the IAV and VSV screens. Amino acid sequences of the obtained anti-IAV **(b)** and anti-VSV **(c)** VHHs are presented (number independent identifications in parentheses).

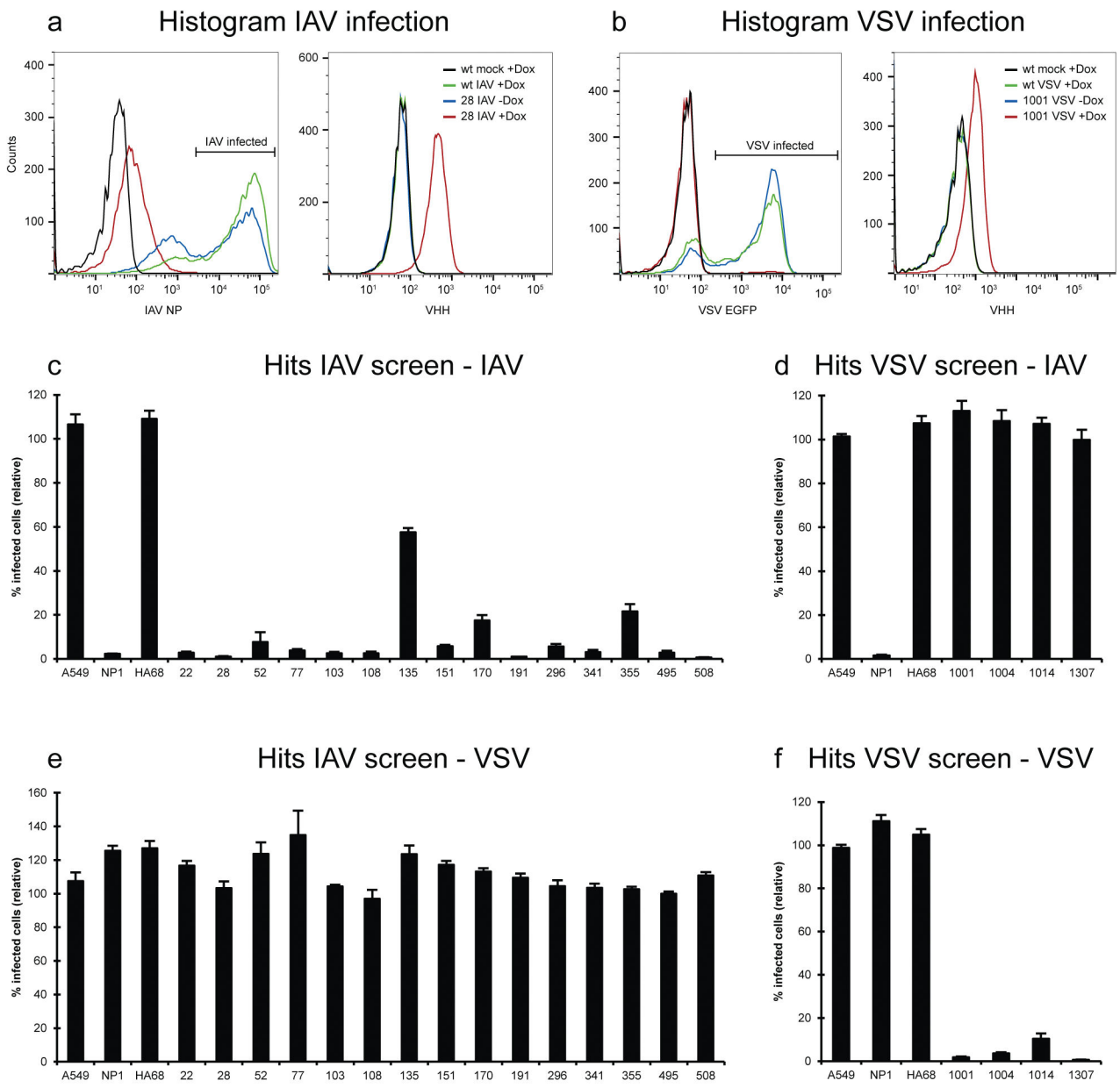

Figure 3.

Validation of antiviral VHHs. A549 cells or clones inducibly expressing the indicated VHHs were treated without or with 1 μg/mL doxycycline (Dox) for 24 h and subsequently infected with IAV WSN **(a, c, d)** or VSV Indiana EGFP[39] **(b, e, f)** for 6 or 4 h, respectively. IAV-infected cells were stained for NP and VHH-HA expression; VSV-infected cells were stained for VHH-HA expression. Cells were analyzed by flow cytometry (sample histograms in **(a)** and **(b)**); the fraction of infected cells in the presence of Dox was quantified and normalized to infection in the absence of Dox. Hits from IAV screen are displayed in **(c)** and **(d)**, hits from VSV screen in **(e)** and **(f)**. All data is from three independent experiments ± s.e.m.

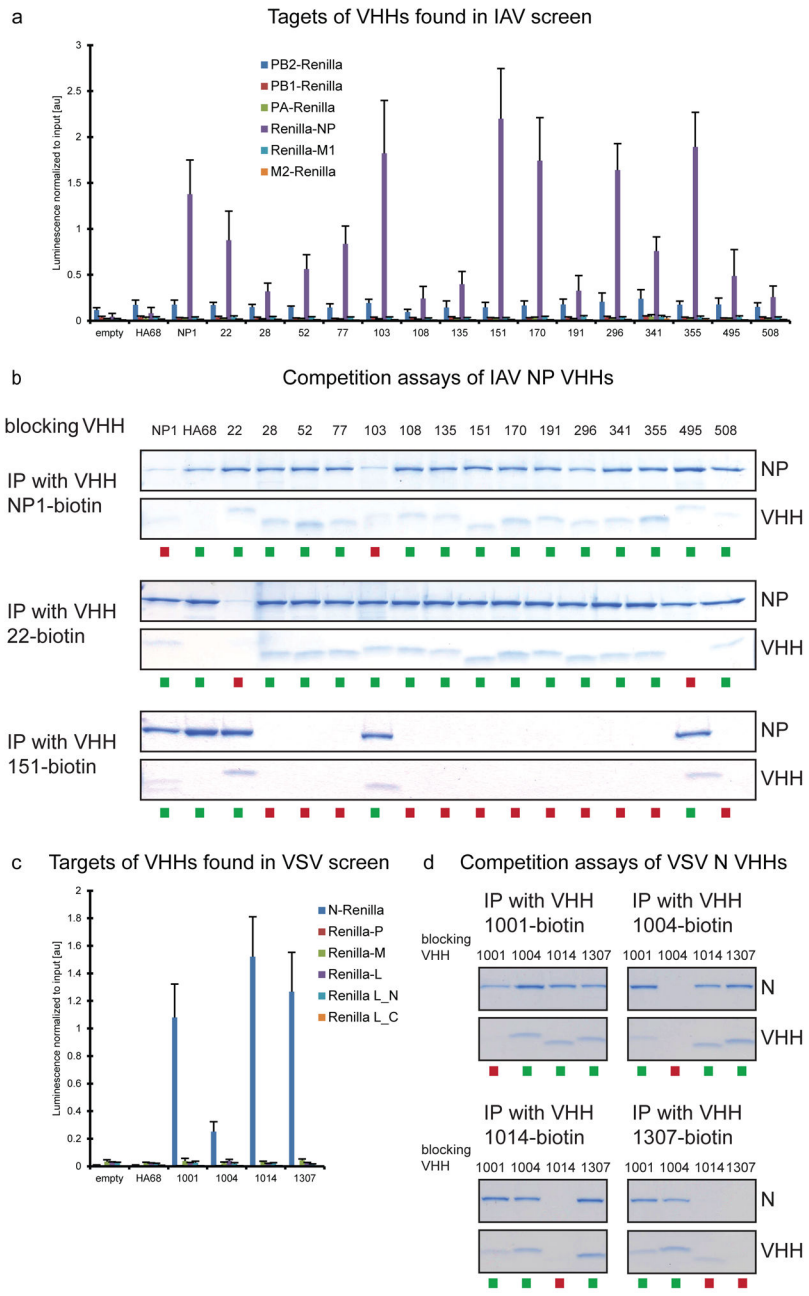

Figure 4.

Identification of VHH targets. **(a, c)** 293T cells were transfected with expression vectors for the indicated HA-tagged VHHs and structural proteins of IAV **(a)** or VSV **(c)** fused to Renilla luciferase. Lysates of the respective cells were incubated with immobilized anti-HA antibodies in 96-well plates. Wells were washed and incubated with Renilla luciferase substrates to measure co-purified luciferase activity. Emitted light was normalized to luciferase activity in the lysate. Data from three independent experiments ± s.e.m. is displayed. **(b,d)** Purified IAV NP **(b)** or VSV N-RNA **(d)** was pre-incubated with the His_6-tagged VHHs indicated at the top and subsequently subjected to immunoprecipitation with

the specified biotinylated VHH. Precipitation of NP/N and the respective VHH was analyzed by SDS-PAGE and colloidal Coomassie staining. Competition due to overlapping binding epitopes of the VHHs is indicated with red squares, successful co-purification with green squares. Representative data from at least three experiments is displayed.

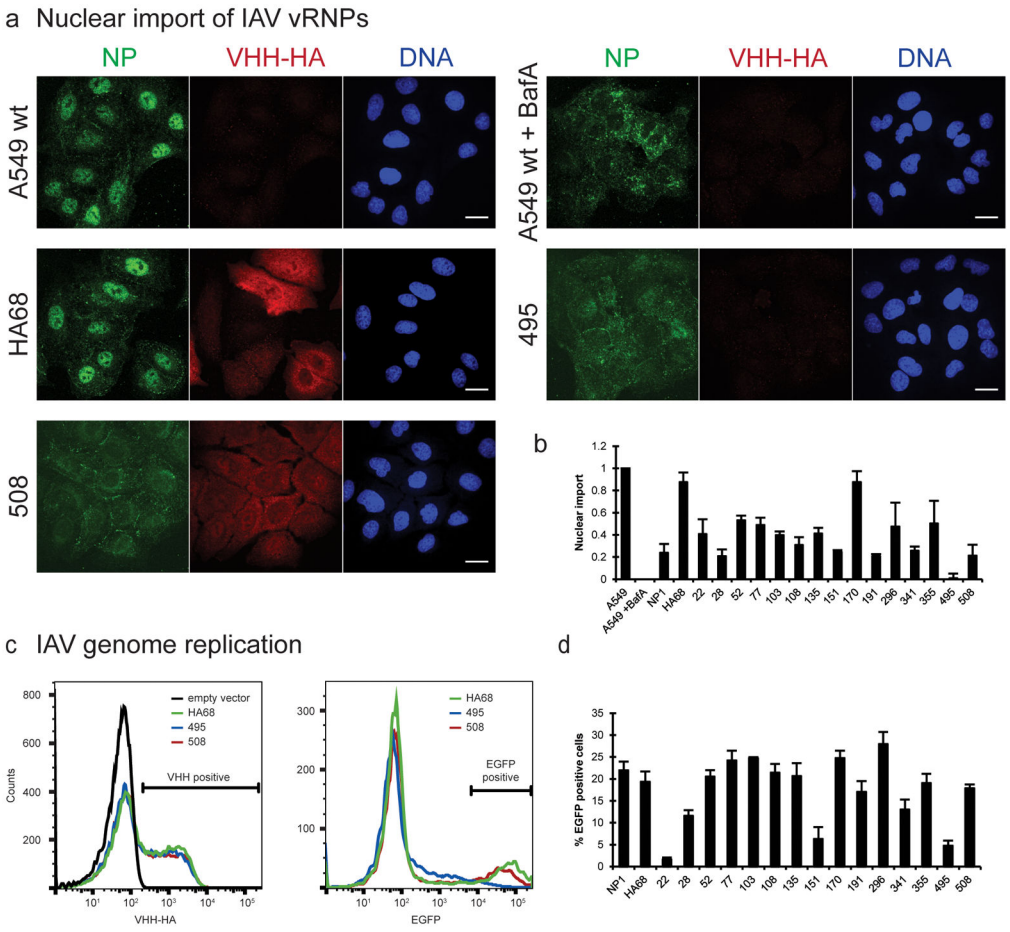

Figure 5.

Anti-IAV VHHs block nuclear import of vRNPs and mRNA transcription. **(a, b)** A549 cells or clones expressing the indicated VHHs were treated with 1 μg/mL Dox for 24 h and infected with IAV WSN (MOI 230) in the presence of 1 mM cycloheximide for 4 h. Controls were treated with 50 nM bafilomycin A1 (BafA). Cells were stained for NP, HA, DNA, and actin; Z-stacks were recorded by confocal microscopy and Z projections of representative examples are displayed in **(a)**. Scale bars represent 20 μm. NP staining in the nucleus and cytoplasm was quantified with CellProfiler and ratios of nuclear/cytoplasmic signal intensities were quantified and normalized to untreated cells (nuclear import = 1.0) and BafA-treated cells (nuclear import = 0). Values from three independent experiments ± s.e.m. are shown. **(c, d)** 293T cells were transfected with expression vectors for IAV WSN PA, PB1, PB2, NP, pPolI-EGFP, and the indicated HA-tagged VHHs. 24 h post transfection, cells were stained for HA and analyzed by flow cytometry. The fraction of VHH-HA-positive cells that expressed high levels of EGFP was quantified. Exemplary histograms are shown in **(c)**, and average data from three independent experiments ± s.e.m. are displayed in **(d)**.

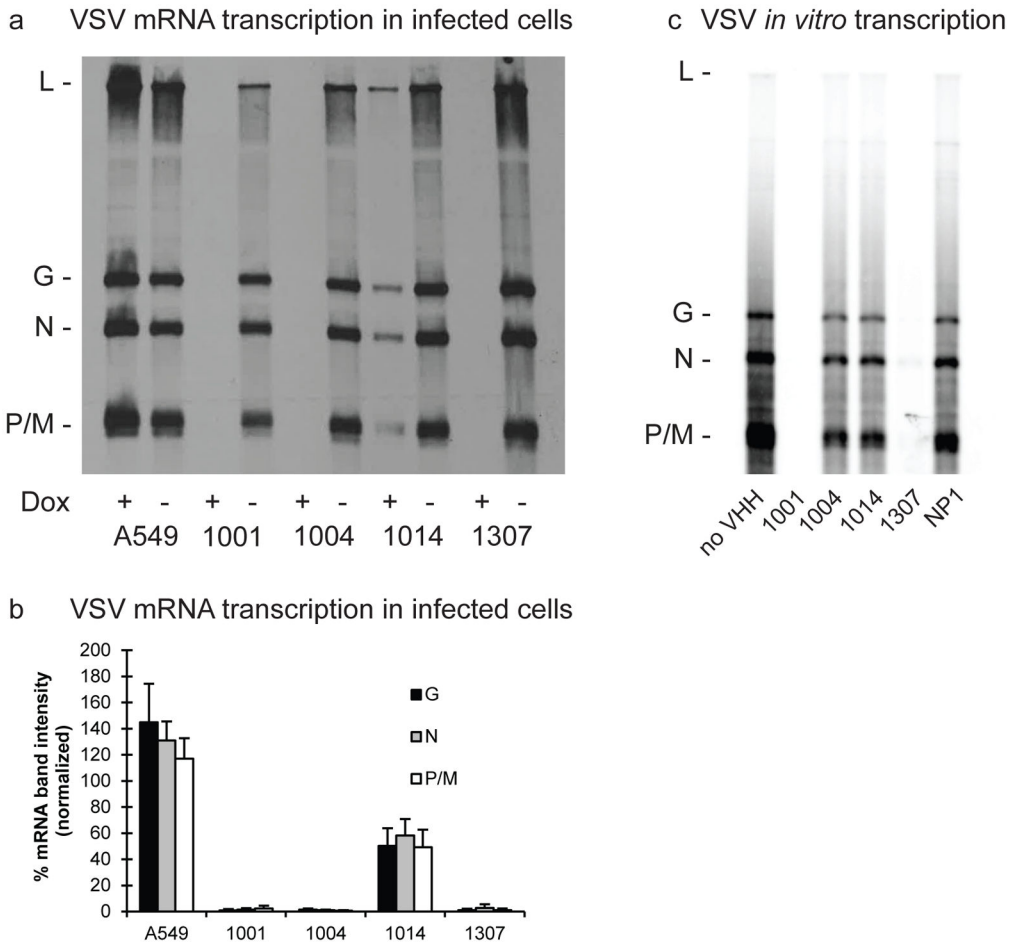

Figure 6.

Anti-VSV VHHs impair mRNA transcription. (**a,b**) A549 cells or clones expressing the indicated VHHs were treated with 1 μg/mL Dox for 24 h, infected with VSV Indiana, and viral RNAs metabolically labeled with [^{3}H]-uridine. We purified the RNA from cell lysates and separated RNA species by acid agarose-urea gel electrophoresis. An autoradiogram representative of three independent experiments is shown; the positions of the mRNAs of the respective viral genes are indicated. Band intensities of G, N, and P/M mRNAs were quantified and normalized to band intensities in the absence of Dox. Average values from three independent experiments ± s.e.m. are shown. (**c**) To test the effects of anti-VSV VHHs on polymerase activity *in vitro*, we incubated recombinantly expressed L and P with N-RNA templates purified form VSV virions. Reactions were performed in the absence or presence of the indicated VHHs as well as NTPs, including [α-^{32}P]-GTP. RNA species were separated by acid agarose-urea gel electrophoresis. An autoradiogram representative of three independent experiments is shown; the positions of the mRNAs of the respective viral genes are indicated.